Electron Holography of Field-Emitting Nanotubes

John Cumings*, M.R. McCartney†, J.C.H. Spence¤, and A. Zettl*

*Department of Physics, University of California at Berkeley, and Materials Sciences Division, Lawrence Berkeley National Laboratory, Berkeley, CA, 94720, USA
†Center for Solid State Science, Arizona State University, Tempe, AZ 85287-1504, USA
¤Department of Physics and Astronomy, Arizona State University,Tempe,AZ85287-1504,USA

Abstract. We have used electron holography performed *in-situ* inside a high resolution transmission electron microscope to determine quantitatively the electric field distribution in and around individual voltage-biased and electron-field-emitting multiwalled carbon nanotubes. The temporal stability of the electric field distribution near the nanotube is also investigated.

Electron holography experiments were performed on multi-wall carbon nanotubes grown by conventional arc-synthesis methods. Individual nanotubes, one end of which was attached to a conducting electrode, were subjected to external voltage bias (with respect to a gold collector plate that was located approximately 6μm away) both below and above the threshold for electron field emission. For various fixed selected bias voltages electron holograms were recorded inside a high-resolution transmission electron microscope (TEM). The holograms were then analyzed to obtain quantitatively direct spatial electric potential and electric field distributions in and around the individual nanotubes.

Our experimental configuration merges the previously demonstrated technique of *in-situ* TEM imaging of nanotubes under electron field emission conditions [1, 2] with that of electron holography [3]. After traversing the nanotube region, the TEM *imaging* electron beam (distinct from the nanotube field-emission electrons) is split by a fine-wire biprism beamsplitter. TEM focusing electronics then converge and overlap the split beams onto a common imaging plane where the holographic fringes are recorded. For the experiments reported here nanotube electron field emission was first significant at a bias of V_b=70 volts (with a field emission current of 40 pA). At V_b=120V the total field emission current was 0.54 μA.

The phase shift ($\Delta\phi$) that an electron acquires traversing a spatially-dependent potential V is given by

$$\Delta\phi = \alpha \int_{\text{beam path}} V dl \qquad (1)$$

CP591, *Electronic Properties of Molecular Nanostructures*, edited by H. Kuzmany et al.

where α is a parameter that depends on the accelerating voltage of the electron microscope. For the present experiments performed with a 200 keV TEM imaging beam, α is 7.29 milliradian per volt-nm.

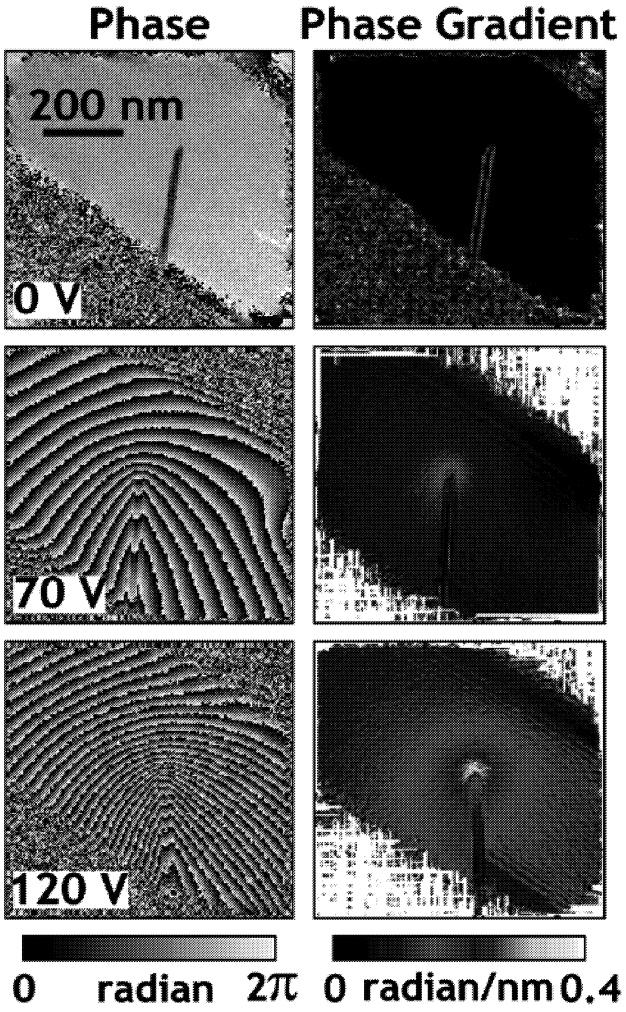

FIGURE 1. Phase shift and phase gradient maps extracted from holograms of the same nanotube at bias voltages V_b =0, 70, and 120V. The phase gradient indicates where the electric field is the strongest; note the concentration of the electric field at the nanotube tip for V_b = 70 and 120V.

Fig. 1 shows in the left-hand column a series of phase shift maps obtained by Fourier transform analysis of hologram images recorded at selected nanotube bias V_b, both below and above the threshold for nanotube electron field emission. The phase shift is plotted in radians on a grayscale from 0 to 2π. The upper phase shift map is for V_b=0, and here the featureless area around the nanotube demonstrates that, in the region surrounding the nanotube, the imaging electron beam has a uniform phase. In this V_b=0 phase shift map the nanotube itself appears (as the 300 nm long vertical stick-like structure near the center of the figure); the portion of the imaging beam that "goes through" the nanotube is shifted by a uniform 3.1 radian from the background phase. This contrast is due to the difference in the integrated potential (Eq. (1)) for the imaging beam inside the nanotube relative to the vacuum potential [3]. From these zero-bias V_b=0 data, we find a mean "inside" potential for the nanotube of 12 volts, in agreement with previous measurements on other carbon materials [3, 4, 5]. The center and lower phase shift maps in the left-hand column of Fig. 1 are calculated from holograms taken at V_b=70 V and V_b=120 V, just above and significantly above the threshold bias for field emission for this nanotube. In these phase shift maps the phase shift due to the applied nanotube bias is strikingly apparent. In these modulo-2π plots, whenever the phase shifts by 2π it wraps back to zero, causing stripes in the phase map. These stripes show the equiphase lines of the hologram.

The right-hand column of images in Fig. 1 represents phase gradient data associated with the phase shift maps just discussed. These phase gradient maps are determined directly from the phase shift maps shown to the left. For V_b=0, the phase gradient is featureless in the region surrounding the nanotube, while for V_b=70V and 120V (in the field emission region), the phase gradient is clearly concentrated at the tip of the nanotube.

The phase shift and phase gradient maps of Fig. 1 are related to, but not direct quantitative representations of, electrical potential and electric field maps, respectively. For example, the lines delineating phase 2π "rollovers" on the left column of Fig. 1 are fair representations of the actual equipotential lines in the region *outside of* the nanotube, and the regions of highly concentrated phase gradient corresponds to regions of high electric field. Within the nanotube and along its length however, the phase shift maps of Fig. 1 show, for V_b=70V and 120V, a series of phase shift 2π rollovers. It is important to note that these rollovers within the nanotube do *not* in themselves imply that the physical voltage is dropping along the length of the nanotube (with implications for ballistic or non-ballistic transport along the tube, for example). The high concentrations of electric field at the tip of the nanotube for V_b=70V and 120V demonstrate that the electric field is most intense at the tip of the nanotube. Even for large nanotube bias voltages, we see no evidence for high concentrations of electric field at other locations along the nanotube length. Since the local electric field dictates nanotube electron field emission, these results imply that nanotube electron field emission occurs only from the tips of nanotubes, not from sidewall defects or other field-concentrating geometrical or electronic irregularities.

To obtain quantitatively the local electric field magnitudes associated with the field emission, further analysis of the holographic information is necessary. We create a model potential (derived from a model charge distribution), which, from Eq. (1),

ultimately yields the correct (experimentally determined) phase shift map. Our model is a one dimensional line of charge [6], with a complementary image charge distribution (due to the induced charges on the gold collector plate). Cylindrical wall geometry of the nanotube, along with the (idealized) hemispherical nanotube cap, is achieved by allowing the linear charge density of the model to be a variable function of position. The model yields phase shift and phase gradient maps which are fit to the experimental data. The electric potential and electric field distributions of the model are then quantitative representations of those parameters for the actual biased nanotube.

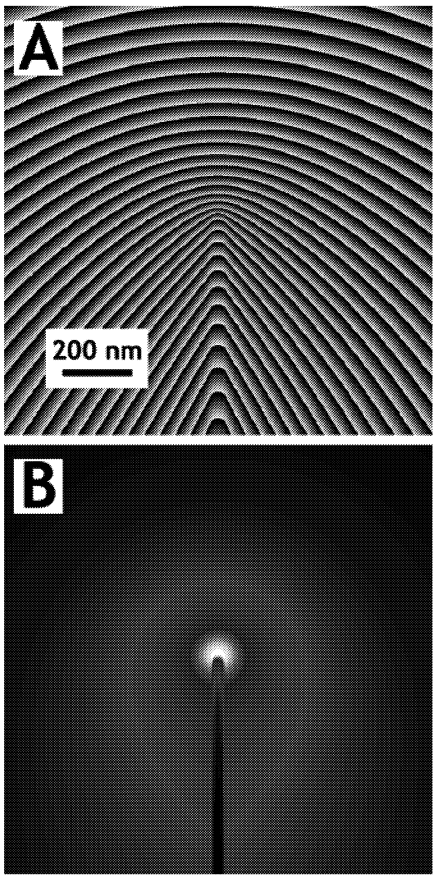

FIGURE 2. Model phase shift (A) and phase gradient (B) for a nanotube with V_b=120V. Part A is the phase and Part B is the phase gradient.

An example of a complementary phase shift and phase gradient map determined by fits to the model are shown in Fig. 2. The model prediction matches closely the data for the field emitting nanotube biased at V_b=120V. The fit yields an electric field strength at the tip of the nanotube E=1.22 V/nm. Electric field strengths at the

nanotube tip were similarly determined for V_b= 90V and V_b=70V and are 0.82 V/nm and 0.64 V/nm, respectively. It is important to note that the nanotube in the model has a constant potential along its length, yet the equiphase lines cut through the nanotube, just as they do in the experimental data of Fig. 1. Therefore, the holography is consistent with no potential drop along the length of the nanotube, even in the strongly field-emitting regime.

We now consider fluctuations. In the field emission regime the nanotube emission current was observed to fluctuate greatly in time. In some cases, the current varied by as much as 80% of its peak value. The fluctuations in current, however, can *not* be attributed simply to fluctuations in the local electric field at the tip of the nanotube. If the phase of the image wave varies during the exposure time of a hologram, then the fringes in a hologram can become blurred. For the current work, 4 second exposure times were used to capture the holograms. If the fluctuations cause phase shifts on the order of π, then the fringes will disappear altogether. From our model of the nanotube phase, we estimate that a fluctuation of only 0.03 V/nm in the strength of the electric field at the tip of the nanotube could cause the fringes to be completely blurred. We therefore conclude that the electric field strength at the tip of the nanotube varied by less than 2.5% during the exposure of the hologram. Therefore, field emission current fluctuations cannot be a mechanism tied to changes in the local electric field magnitude or distribution (for example unraveling of the nanotube fabric at the tip or strong fluctuating intertube interactions). It is far more likely that subtle tip electronic structure, as might occur with tip adsorbates [7], alter the emission current without significant changes in the local electric field strength.

ACKNOWLEDGEMENTS

John Cumings and A. Zettl acknowledge support by the Director, Office of Energy Research, Office of Basic Energy Sciences, Division of Materials Sciences, of the U. S. Department of Energy under Contract No. DE-AC03-76SF00098, and by NSF Grants DMR-9801738 and DMR-9501156.

REFERENCES

1. Wang, Z. L., Poncharal, P., and de Heer, W. A., *Microscopy and Microanalysis* **6**, 224 (2000).
2. Wang, Z. L., Poncharal, P., and de Heer, W. A., *Journal of Physics and Chemistry of Solids* **61**, 1025 (2000).
3. Völkl, E., Allard, L. F., and Joy, D. C., *Introduction to electron holography* Kluwer Academic/Plenum Publishers, New York, 1999.
4. Lin, X. and Dravid, V. P., *Applied Physics Letters* **69**, 1014 (1996).
5. Tonomura, A., Electron holography : proceedings of the International Workshop on Electron Holography, Holiday Inn World's Fair, Knoxville, Tennessee, USA, August 29-31, 1994. Elsevier, Amsterdam ; New York, 1995.
6. Matteucci, G., Missiroli, G. F., Muccini, M., et al., *Ultramicroscopy* **45**, 77 (1992).
7. Dean, K. A. and Chalamala, B. R., *Applied Physics Letters* **76**, 375 (2000).